A snake-like robot for internal inspection of complex pipe structures (PIKo)

Sigurd A. Fjerdingen, Pål Liljebäck and Aksel A. Transeth

Abstract— **This paper presents a mechanism for navigating complex pipe structures, both horizontally and vertically. The mechanism consists of a series of identical modules interconnected by two degree of freedom active joints. A set of active wheels on each module provides propulsion. Horizontal motion is achieved through a train-like scheme, while vertical motion is achieved through spanning the pipe alternatingly with the modules. The design and the capability of horizontal and vertical motion is validated through experiments.**

I. Introduction

Inspection, maintenance and repair (IMR) of pipelines have in recent years gathered focus from a diverse group of researchers. One important reason for this is that there is an emerging need for IMR while keeping costs down in several thousand kilometers of 30 to 50 years old sewer lines [11], energy delivery systems in countries such as the United States, and other pipe-like structures such as ventilation systems [2]. This paper addresses some of these issues by proposing a transport mechanism able to navigate and inspect complex pipe-like structures without the necessary precondition of shutting the process down. The proposed design draws upon past experiences from the very flexible and adaptable snake-like robots, and at the same time specializing the design for a specific environment – namely pipelines and other pipe-like structures.

Several designs have been proposed for snake-like robots. The earliest snake-like robot, called ACM III, was developed by Hirose in 1972 [6]. The ACM III was equipped with passive wheels and sinus-like movements of the robot body was used to obtain the necessary propulsive force for propelling the snake robot forward. Other snake robot designs with passive wheels have also been proposed [3],[7]. Moreover, several snake robots without wheels have been developed [8],[9]. However, none of these designs are directly applicable to pipe-inspection as they do not consider the constrained and longitudinal nature of pipelines. To this end, *active* wheels are beneficial for moving within pipes. Yamada and Hirose developed a water-proof snake robot with active wheels called ACM-R4 in 2006 [10]. They showed that such a mechanism has a feasible locomotion principle and interesting methods for horizontal motion control. Methods for moving the snake robot from one horizontal plane to another were developed and tested with experiments. However, the robot motions were timed and pre-coded. In addition, purely vertical motion was not displayed. The OmniTread is a similar robot employing crawler threads instead of wheels [14]. Experiments have shown the ability to climb vertically, using three operators simultaneously to perform motions.

Sigurd A. Fjerdingen, Pål Liljebäck and Aksel A. Transeth are with SINTEF ICT Dept. of Applied Cybernetics, N-7465 Trondheim, Norway.
E-mail: {Sigurd.Fjerdingen, Pal.Liljeback, Aksel.Transeth}@sintef.no

Fig. 1. The pipe inspection robot PIKo.

More application specific robot designs have also been proposed. In particular, inspection of sewer systems and gas pipelines has attracted attention. The MAKRO project developed a serially connected robot with active wheels designed for sewer inspection [12]. The robot was able to move horizontally and, to some degree, from one horizontal plane to another by lifting parts of the body at a time. For gas lines, the MRINSPECT robot was claimed to be able to move through bends both horizontally and vertically [13], but it lacks the sought generality as each module needs to be able to span the entire pipe diameter.

Many interesting robots for navigating pipe-like structures have been proposed. However, the application specific designs presented limit the range of application to either horizontal pipe structures or vertical/horizontal pipe structures with particular requirements to pipe diameter and/or pipe layout. For example, robots have been developed to traverse vertical pipe segments. However, their designs restrict them from being capable of moving upwards in T-junction or handling pipe structures with large differences in pipe diameters.

This paper presents a design and implementation of an articulated transport mechanism with active wheels and joints for locomotion in pipe structures with varying dimensions and complex structural configuration. Moreover, a novel design for both measuring contact forces between the robot and its environment, and the bilateral constraint forces between adjacent robot modules are presented. The choice and integration of sensors and actuators are well documented in order for others to re-use the proposed technical solutions. Experimental results verify that the transport mechanism is capable of both horizontal turning motion and vertical climbing inside a pipe-segment. More elaborate work on control and navigation strategies for in-pipe inspection is beyond the scope of this paper.

The paper is organized as follows. Section II gives an

overview of the design and capabilities of the transport mechanism, while Section III describes more closely how the joints and wheels are actuated. Section IV details the motion control system and the various on-board sensors, and experimental results are given in Section V. Section VI contains conclusions and further work.

II. Overview of the Design

The goal for the robot design presented in this paper has been to make navigation in complex pipe structures of varying diameter possible. By complex, we mean structures of pipes consisting of straight segments in both the horizontal and vertical direction – possibly of varying diameter, together with bends and T-joints of varying radii. Additionaly, the mechanism should be able to traverse varying kinds of obstacles, such as constrictions from valves. The proposed mechanism draws on earlier designs in the field and expands on them by being more robust with respect to varying pipe diameters and junction traverses.

The main principle of actuation stem from more generic snake-like robots. The mechanism, shown in Fig. 1, consists of a series of identical modules interconnected by two rotational joints on both sides of the modules. Additionally, wheels on each module provide forward and backward propulsion. All degrees of freedom are actuated, as opposed to many snake-robot designs with passive wheels. Currently, five modules have been connected, and this has proven sufficient for horizontal and vertical motion.

Horizontal movement is achieved in a conceptually similar manner of a train moving on tracks. The idea behind vertical movement is to use the flexibility of the interconnected joints to push against two opposing sides of the pipe at the same time, while moving forward by propulsion from the wheels. This principle of movement is shown in Fig. 2. Both principles adjust to an arbitrary diameter pipe under the assumption of the existence of enough interconnected modules. The following sections will detail the design and motion strategies of the pipe inspection robot.

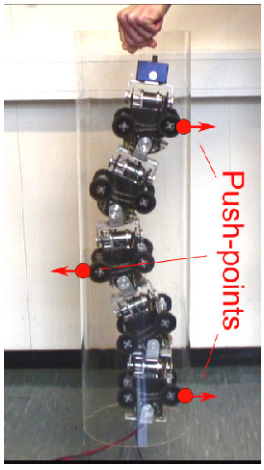

Fig. 2. Scheme for vertical climbing. The robot uses push-points on each side of the pipe to mount itself.

III. The Actuation Mechanism

As illustrated by Fig. 3, each module has two degrees of freedom relative to its neighbouring modules. One joint controls the yaw and connects the module to its previous neighbour. The other controls the pitch and connects the next neighbour in the series. Also illustrated in Fig. 3 are the special forks connecting the modules.

A module consists of an assembly, shown in Fig. 4, and an outer aluminum housing. The main parts of the assembly are three Hitec servo motors (HS-5955TG), each responsible for actuating one degree of freedom, and two Faulhaber planetary steel gears (series 32/3 S) of ratio 1:14. Steel roller chains connect the two motors actuating the joints to the gears. The gear shaft is connected to the fork via a custom fork ear, as shown in Fig. 5(b). The motor responsible for wheel rotation is connected via a custom shaft locking mechanism, as shown in Fig. 4 and Fig. 5(a). All four wheels are connected mechanically in such a way that one servo motor synchronously drives all the wheels.

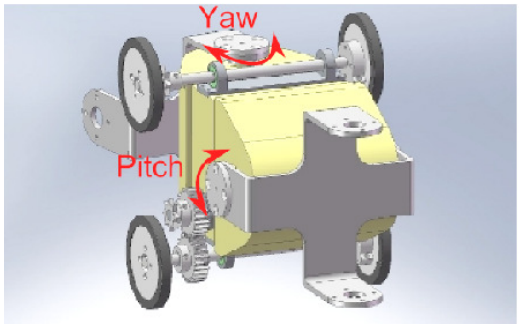

Fig. 3. Illustration of the joint articulation scheme. Pitch and yaw changes the rotation of the forks, and the wheels are synchronously driven.

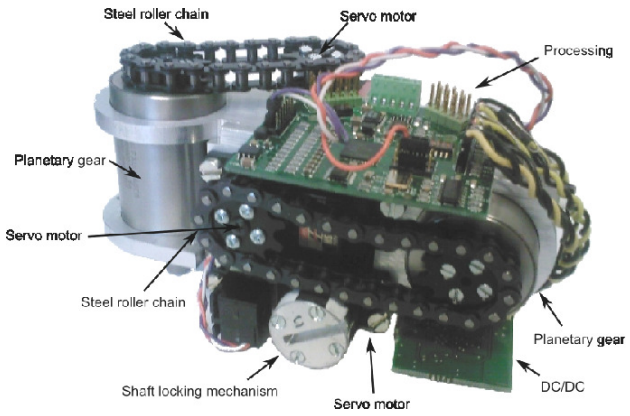

Fig. 4. The internal assembly of a module.

Servo motors are manufactured to have a limited range of motion, but by manually modifying the motors continuous rotation is achieved. This process is detailed by Liljebäck et al [1].

Experiments indicate a maximum continuous torque from the servo motors of about 1.6 Nm at 6V supply voltage [1]. Experiments with the assembled joint modules indicate that

(a) Shaft locking mechanism. (b) Fork ear for shaft coupling.

Fig. 5. Mechanical components for wheel rotation and joint articulation.

Weight of module	1.252 kg
Length between joint axes	0.150 m
Max joint travel	$\pm 75°$
Max continuous joint torque	11.5 Nm
Max joint speed	$28°/s$
Module width	0.130 m
Module height	0.140 m

TABLE I

PARAMETERS FOR A MODULE.

each joint (servo motor and external gear) has a maximum joint torque of about 11.5 Nm. The theoretical upper bound is computed to be 17.9 Nm given the rated power efficiency of 80% by the gears. The discrepancy is probably due to friction in the chain drive and shaft connection to the forks. A module weighs 1.252 kg and the length between consecutive joint axes is measured to be 0.15 m. This means that each module is able to lift at least three consecutive modules (more if module lifting is performed in a cascading fashion to move the center of mass iteratively closer to the point of rotation). Lifting of three modules has been verified by experiments. Table I lists essential parameters characterizing the actuation system.

IV. Control and Perception

A. Control System

Each module is controlled by a custom-designed micro-controller board based on the Atmel AT90CAN128 MCU, shown in Fig. 6(a). The board controls the servo actuators and has several analog and digital input ports for various sensors described in the following sections. Each module also has a custom-designed power supply board, shown in Fig. 6(b), converting from the 30 V running through the entire robot to the 6 V needed by the servo motors. This is done to reduce the amount of current needed in the power supply wires interconnecting the modules.

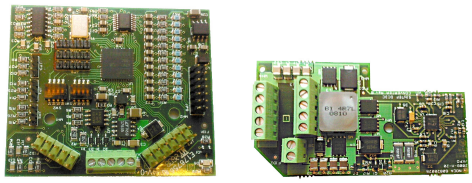

(a) Module controller board. (b) DC/DC board.

Fig. 6. Printed circuit boards implemented in each module.

The module controller boards run on a separate 5 V power supply to avoid unintentional operation resulting from disturbances and high current drain spikes from the servos. Experiments with the servos have indicated an in-rush current of about 9 A at 6 V. The module controllers communicate with a master over a CAN-bus, as illustrated by Fig. 7. The master is a TS-7800 ARM-based embedded controller from Technologic Systems. The master controller runs Debian Linux. It is connected to a Peak PCAN USB dongle for CAN-communication with the other modules, and a D-Link DWL-G122 WiFi-G USB dongle for wireless UDP/IP communication with an external PC. The PC has an Xbox 360 gamepad connected, which is used to control the robot.

The UDP protocol is unreliable in that packages may be lost, duplicated, or arrive out of order. This application is, however, considered to be time-critical in that it is preferrable to drop packages arriving too late – especially when it comes to observations from the robot. The newest data is considered to be the best data, and old data arriving late is discarded. This is implemented via an incrementing counter in the messages. Commands from an external PC going to the robot may also be lost, which is not explicitly handled in the software. Here it is assumed that feedback to the operator from the observed robot is adequate for compensating such losses. It may be equally bad for control to receive a command too late, as would be the case when loosing an initial message in a protocol such as TCP, as not receiving the command at all.

The master controller is currently physically residing outside the robot, as indicated by Fig. 7, and there is an external set of CAN bus wires running in parallel with the power and signal power supply wires. Future work will physically integrate the master controller in the head module of the robot.

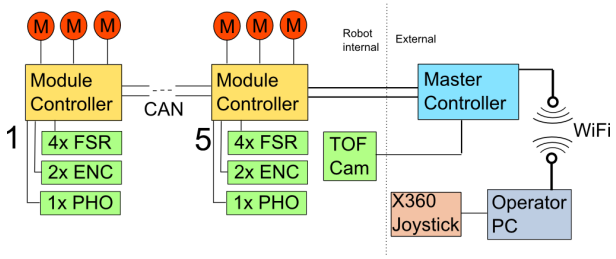

Fig. 7. Overview of the control system.

Each module controller runs local PI-regulators for position control of the joints, and a simple P-regulator for speed control of the wheels. Sensor and status information is sent to the master using a subscription-based protocol. The main task of the master controller is to convert high level commands from the gamepad to correct angle and speed values of each module. Joystick commands sent from the external PC are currently adjusting two high-level parameters: The reference wheel speed of the robot and the reference curvature of the path the robot should follow. The algorithm for curve following is described in section IV-D.

B. Proprioception

The robot employs three main methods for measurement of the internal states, namely (a) absolute angle measurements of the joint angles, (b) relative measurements of the wheel angles – known as odometry, and (c) current drain measurements for the servo motors. Fig. 8 and 9 shows the method and placement of the joint angle sensors, respectively. Each module is equipped with two magnetic encoders (Fig. 8(a)) from Austriamicrosystems (AS5043), and a custom fork ear with a mounted magnet (Fig. 8(b)). In total, as shown in Fig. 9, this gives the possibility of measuring the angle of the fork, i.e. the neighbouring module, in relation to the module in question. Output from the magnetic encoders has 10 bit resolution and is used as feedback for the PI-controllers in the module.

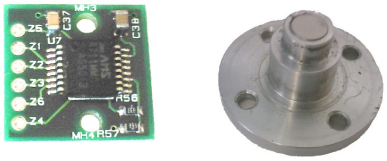

(a) Magnetic encoder. (b) Fork ear and magnet.

Fig. 8. Joint angle measurement components. The fork ear with magnet rotates over the magnetic sensor.

As previously stated, the relative angle of the motion of the wheels is also measured. This is handled by an OPTEK photoreflector (OPB716Z) in combination with an alternating pattern of black and white mounted on the shaft locking mechanism. The black and white pattern can be seen on Fig. 4. Dead reckoning schemes such as this will lead to accumulated position errors over time. The robot currently consists of five modules, each with its own dead reckoning count, which further adds to the complexity. Slipping of the entire robot will cause errors, as well as resolution approximations due to the nature of the sensor readings. To correct accumulated errors, the odometry readings should be fused with information from the 3D camera. This has not been implemented.

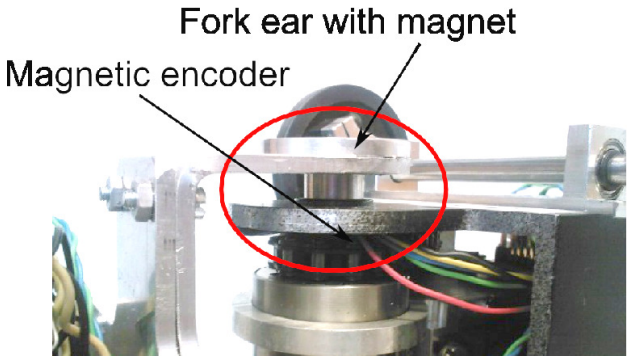

Fig. 9. Placement of the magnetic encoder in relation to the magnetic fork ear.

The current through each motor is measured by feeding the current through a $0.025\ \Omega$ precision power resistor from Vishay Dale and measuring the resulting voltage drop over this resistor. The measurement setup is shown in Fig. 10. These measurements are used as an internal safety mechanism to stop the motors from overheating, which may happen when stalling for prolonged periods of time.

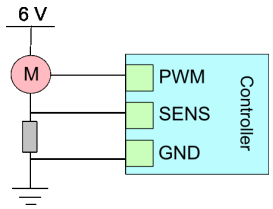

Fig. 10. Sensor setup for current sensing resistor.

C. Exteroception

Several aspects of the environment need to be perceived by the robot in order to make it suited for navigating pipe structures. Firstly, there is a need to percieve key navigational geometries in the environment. In pipe structures, these will typically be bends, junctions, and pipe radius, as well as possible obstacles. The robot is equipped with a 3D time-of-flight (TOF) camera from Mesa Imaging (SR3000) for this purpose. The method used for tracking of pipeline features implemented on the robot has been presented by Thielemann et al [5], and will not be detailed here. The central idea of the algorithm is to group pixels deviating from an estimated cone into regions, and then track regions fulfilling constraints on shape and stability over time. This gives a representation of features not recognized as the pipe itself, and enables further processing on what kind of object the identified feature is.

Secondly, we wish to be able to measure the amount of force that the robot is exerting on its environment. Reasons for such measurements include the ability to detect situations in which the robot is stuck, in which case an opposing force from the environment will be detected, but first and foremost the measurements are useful in regard to the motion scheme for vertical climbing, as detailed further in section IV-D. The purpose of this section is to present the sensor setup. Experimental validation of aspects of this setup will be subject for future work.

Each fork connecting two modules is divided into two parts fastened rigidly by eight screws. The divided fork is shown in Fig. 11. On each end of the fork a force sensing resistor (FSR) is mounted. There are a total of four FSRs mounted on each fork. FSRs have already been used in several snake-robot designs [1],[3],[4]. A FSR is a polymer device which increases internal conductance (1/resistance) approximately proportionaly to the amount of force exerted on the active surface area. It is not suited for accurate measurements as it is considerably effected by hysteresis and temperature. It is, however, well suited for measurements of a more qualitative manner, such as a coarse division of applied force into e.g. *severe, high, low, none*. This makes the FSRs well suited for the needs of the current design,

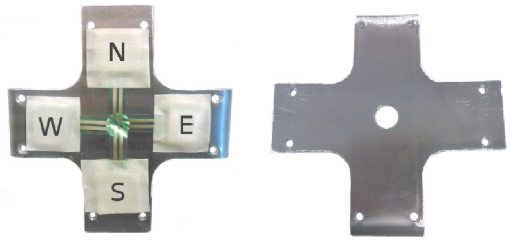

Fig. 11. Divided fork with FSRs installed. The forks connect each module to its neighbour.

where the main requirement is to sense whether a module is being pushed against an opposing surface.

The FSRs used in the forks have an active area of 13 mm in diameter, and one is shown in Fig. 12(a). A compliant material (rubber adhesive) is mounted over each FSR. This will distribute the forces over the entire surface area of the FSR. The setup is shown in Fig. 12(b). The sensor setup is similar to earlier work on force sensing in snake-like robots [1],[4], but is applied in a novel way by using the interconnection between modules instead of directly sensing the forces acting on each module.

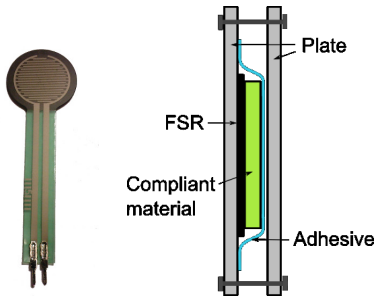

(a) FSR. (b) FSR setup on fork.

Fig. 12. Sensor setup for measuring contact forces in forks.

The FSR arrangement makes it possible to detect three different kinds of forces: Horizontal and vertical forces resulting from rotational moment, and tension forces from pushing or pulling one module in relation to a neighbour. These three groups of forces are shown in Fig. 13.

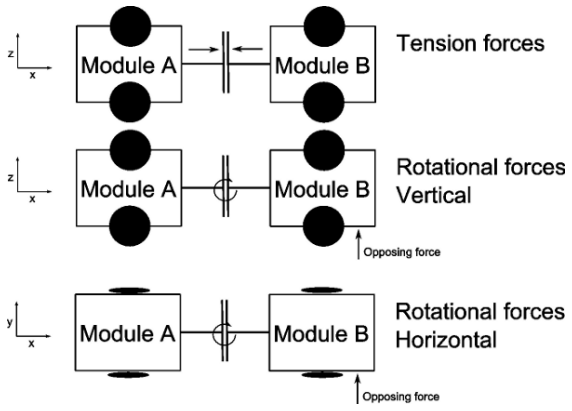

Fig. 13. Forces measured by FSR setup.

In order to calculate the tension force, the mean of all four FSRs are used. For the horizontal rotational force, the difference between the FSR marked E and W is used, and for the vertical rotational force, the difference between N and S is used.

D. Principles of Motion

As mentioned in the design overview, there are two main principles of motion; one for horizontal and one for vertical motion. For horizontal motion, a *follow-the-leader* approach is used. This approach is based on the principle that all following modules repeat the pattern of the first module (the leader) at the exact same spatial position as the leader module executed the pattern. More formally stated in a recursive manner

$$\alpha_i(s = s + \Delta s) = \alpha_{i-1}(s), \qquad i \in [1, N] \tag{1}$$

where α_i describes the relative horizontal angle of module i in relation to its next neighbour, Δs is the distance in s between module i and $i-1$, s the curve traced by the longitudinal direction of the robot modules, and N is the number of modules. This motion will result in a train-like movement of the modules. The synchronous wheels will introduce slip, and thereby inaccurate odometry measurements. These errors are alleviated somewhat by utilizing a voting scheme on the distance travelled. If there are discrepancies between travelled distance read by the different modules, the majority vote will be used as the actual outcome. The underlying assumption for correctness is that more than half of the modules are in non-slip condition at all times, an assumption that necessarily will not hold in all conditions. Inaccuracies due to the limited resolution of the photoencoder and pattern combination are not catered for.

For vertical motion, the same follow-the-leader scheme is used, but the output from this motion primitive is interpolated with a primitive that tries to push alternating parts of the robot against the floor and roof of a structure. Fig. 2 shows the result of this primitive. For the general idealized case of a robot with N modules of length L, where maximum vertical angle between two consecutive modules is defined as ϕ_{max}, the number of modules in each pushing and spacing segment, N_{seg}, should be selected such that $\phi \leq \phi_{\text{max}}$, as illustrated by Fig. 15. N_{seg} may be approximated by calculating

$$e = r - r\sin(\cos^{-1}\left(\frac{W}{2r}\right)) \tag{2}$$

and inserting into

$$N_{\text{seg}} \geq \frac{2r - H - 2e}{L\sin(\phi_{\text{max}})}, \qquad N_{\text{seg}} \in \mathbb{N}_1 \tag{3}$$

where W is the module width, H the module height, r the pipe radius, L the module length, and e as indicated in Fig. 14. With reference to Fig. 15, note that at least three pushing segments are needed in order to create a stable opposing-push, whereas only two of the necessary pushing segments are shown. Feedback fom current sensing resistors are used to stop the motion from progressing if the current into the

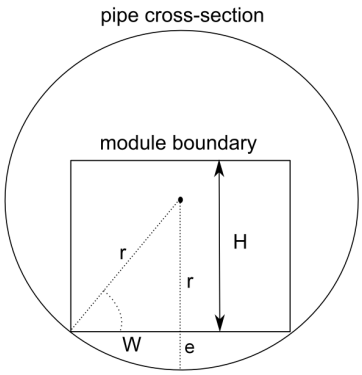

Fig. 14. Pipe cross-section.

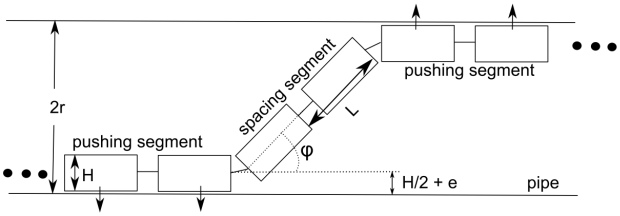

Fig. 15. Pipe longitudinal section showing how the opposing-push scheme works conceptually.

servo motors is too high, which may lead to overheating of the motors. Fig. 16 shows the conceptual layout of the joint control for this scheme.

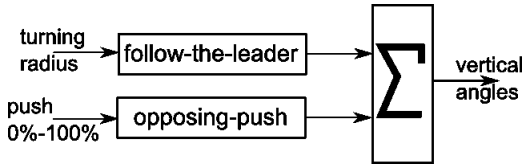

Fig. 16. Conceptual scheme for vertical motion.

V. Experimental Validation of the Design

This section presents experimental results validating the two main principles of motion, namely (a) horizontal motion through a bend, and (b) vertical motion. The purpose of these experiments are proof-of-concept, i.e. to show that the motion primitives described as necessary for sufficient freedom in various pipe structures are actually plausible. At this point in time, it has therefore not been considered important to measure and present factors such as precise path-following abilities and contact force measurements. These features will be the basis of further research, and the results have therefore been limited to sequential images proving the aforementioned concepts.

A. Horizontal motion through bend

The experiment was conducted by creating a virtual bend by installing wall markers on a flat surface, and then steering the robot through the virtual bend by joystick control while taking sequential snapshots with a camera. The bend geometries are given in Fig. 19.

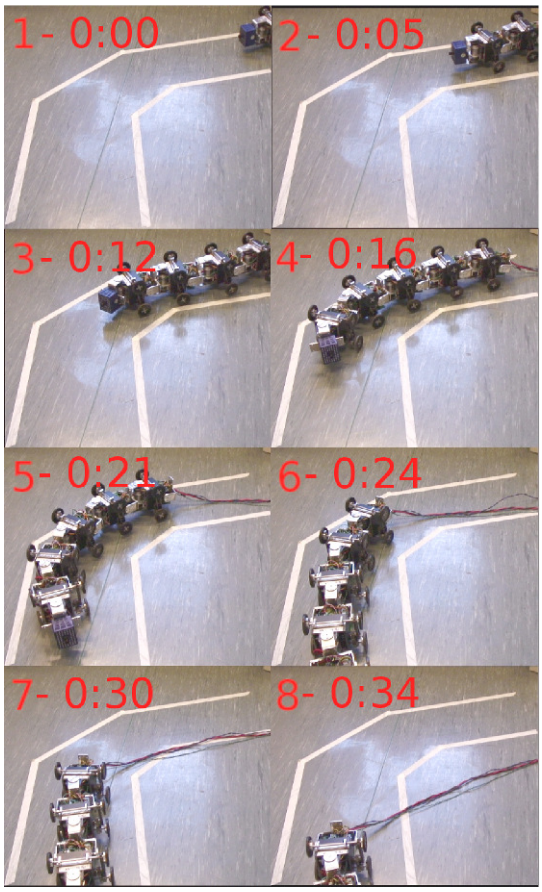

Fig. 17. Experimental validation of horizontal motion through a bend. The numbers in red indicate the frame index and respective min:sec of capture.

Results from the experiment indicate that the follow-the-leader scheme is capable of making the robot act as a train in conjunction with measurements from wheel odometry. Results are shown in Fig. 17.

B. Vertical climbing

The experiment was conducted by inserting the robot in a pipe segment of 0.24 m in diameter made of a transparent plastic material. With the robot inside, the segment was manually tilted vertically while joystick control provided the inputs to the behaviors of pushing against opposing walls and driving forwards. Control of the robot is issued by direct joystick commands, and the amount of pressure applied from the robot to the opposing surfaces is thereby directly controlled by the operator. Hence, measurements from the FSR system mentioned in section IV-C has not been included in this experiment.

Results indicate that the robot is capable of propelling itself vertically. This is shown in Fig. 18. There are two conclusions to draw from this: (1) the opposing-push scheme creates a sufficient friction force between the pipe and the wheels to propel the robot, and (2) the motors driving the wheels are strong enough to cooperatively propel the robot.

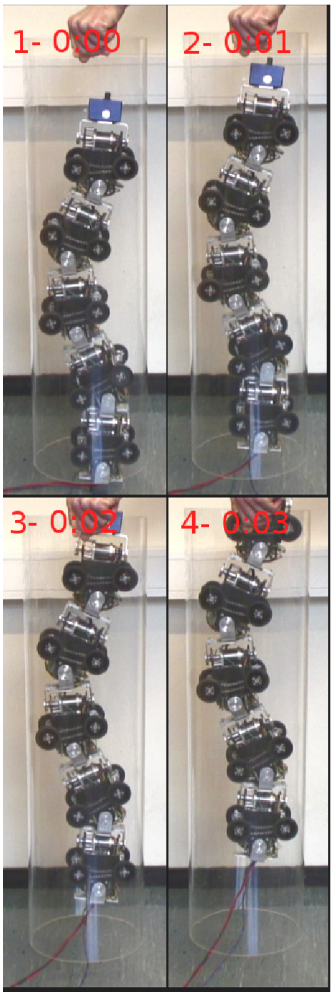

Fig. 18. Experimental validation of vertical climbing. The numbers in red indicate the frame index and respective min:sec of capture.

VI. Conclusions and Further Work

This paper has presented a novel design and implementation of a versatile snake-like robot with active wheels. Moreover, a robust and simple strategy for measuring contact forces between the robot modules and the environment has been proposed.

The mechanism design enables the robot to perform both horizontal and vertical locomotion inside pipe-like structures. To this end, experimental results show that the mechanism is indeed capable of such motion. In particular, experiments showed that the robot is able to move up and down inside a vertical tube. Moreover, the serially connected body of homogeneous modules makes the robot easy to expand in order to enable locomotion within pipes and pipe-like structures with large and/or varying diameters and dimensions by simply adding more modules to the robot.

Mechanisms which are able to move through a diverse set of pipes and pipe-like structures for inspection, maintenance and repair (IMR) have the potential of greatly reducing costs and improving the quality and possibilities of such operations. The experimental results given in this paper show that a snake-like robot is a feasible step towards developing such an IMR mechanism.

Further work will include research on methods for force-measurement-based vertical motion and generalized motion and navigation strategies in pipes and pipe-like structures, as well as fusing environmental observations by the 3D camera, as presented in [5], with measurements from odometer sensors and FSRs.

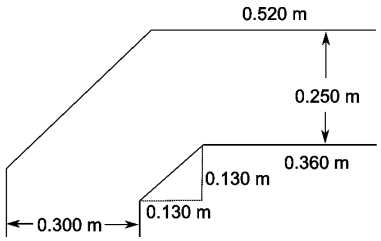

Fig. 19. Experimental setup for the horizontal bend experiment.

References

[1] P. Liljebäck, S. Fjerdingen, K. Y. Pettersen, and Ø. Stavdahl, "A snake robot joint mechanism with a contact force measurement system", in *Proc. IEEE Int. Conf. Robotics and Automation*, May 2009, pp. 3815-3820.

[2] W. Panfil, P. Przystalka, and M. Adamczyk, "Behavior-based control system of a mobile robot for the visual inspection of ventilation ducts", *Recent Advances in Mechatronics*, Springer Berlin Heidelberg, Part 1, pp. 62-66, 2007.

[3] P. Liljebäck, Ø. Stavdahl, and A. Beitnes, "SnakeFighter - development of a water hydraulic fire fighting snake robot", in *Proc. IEEE Int. Conf. Control, Automation, Robotics, and Vision*, December 2006, pp. 1-6.

[4] S. A. Fjerdingen, J. R. Mathiassen, H. Schumann-Olsen, and E. Kyrkjebø, "Adaptive snake robot locomotion: A benchmarking facility for experiments", in *European Robotics Symposium 2008*, vol. 44, pp. 13-22, 2008.

[5] J. T. Thielemann, G. M. Breivik, and A. Berge, "Pipeline landmark detection for autonomous robot navigation using time-of-flight imagery", in *Computer Vision and Pattern Recognition Workshops, 2008, IEEE Computer Society Conference on*, June 2008, pp. 1-7.

[6] S. Hirose, *Biologically Inspired Robots: Snake-Like Locomotors and Manipulators.* Oxford: Oxford University Press, 1993.

[7] A. A. Transeth, R. I. Leine, C. Glocker, K. Y. Pettersen, and P. Liljebäck, "Snake robot obstacle aided locomotion: Modeling, simulations, and experiments", *IEEE Trans. Robot.*, vol. 24, no. 1, pp. 88-104, 2008.

[8] C. Ye, S. Ma, B. Li, H. Liu, and H. Wang, "Development of a 3D snake-like robot: Perambulator-ii", in *Int. Conf. on Mechatroncis and Automation*, August 2007, pp. 117-122.

[9] K. Togawa, M. Mori, and S. Hirose, "Study on Three-Dimensional Active Cord Mechanism: Development of ACM-R2", in *Proc. IEEE/RSJ Int. Conf. Intelligent Robots and Systems*, vol. 3, November 2000, pp. 2242-2247.

[10] H. Yamada, and S. Hirose, "Development of Practical 3-Dimensional Active Cord Mechanism ACM-R4". in *Journ. Rob. Mechatron.*, vol. 18, no. 3, pp. 305-311, 2006.

[11] F. Kirchner, and J. Hertzberg, "A Prototype Study of an Autonomous Robot Platform for Sewerage System Maintenance", in *Auton. Robots*, vol. 4, pp. 319-331, 1997.

[12] K.U. Scholl, V. Kepplin, K. Berns, and R. Dillmann, "An Articulated Service Robot for Autonomous Sewer Inspection Tasks", in *Proc. IEEE/RSJ Int. Conf. Intellingent Robots and Systems*, vol. 2, October 1999, pp. 1075-1080.

[13] S. G. Roh, S. M. Ryew, J. H. Yang, and H. R. Choi, "Actively Steerable Inspection Robots for Underground Urban Gas Pipelines", *Proc. IEEE Int. Conf. Robotics and Automation*, vol 1, 2001, pp. 761-766.

[14] J. Borenstein, and M. Hansen, "OmniTread OT-4 Serpentine Robot - New Features and Experiments", in *Proc. SPIE Defense and Security Conf., Unmanned Systems Technology IX*, May 2007.